Eye-safety analysis of current laser-based scanned-beam projection systems

Edward Buckley (SID Member)

Abstract — Scanned-beam projection systems have attracted much interest recently, with claimed advantages including power efficiency and potential miniaturization consistent with embedding in mobile devices. However, the laser-safety classification and concomitant performance implications, which are arguably the most important issues pertaining to this technology, remain widely misunderstood. In this paper, Class 1 and 2 laser-safety radiometric image power limits for scanned-beam systems are derived with reference to the IEC 60825-1 standard. By calculating the equivalent photometric measure of luminous flux, it is possible to show that the brightness limits for scanned-beam projection systems using current technology are approximately 1 and 17 lm for Class 1 and 2 safety classifications, respectively.

Keywords — *Laser, safety scanned beam, projection.*

DOI # 10.1889/JSID18.11.944

1 Introduction

Laser-based light engines are beginning to emerge as a candidate technology for powering so-called "pico-projector" products, which are characterized by battery operation and output luminous flux values of less than 50 lm. In theory, laser-based light engines offer some attractive features and benefits, since they can exhibit a small factor, long depth of field, polarization independence, and potentially higher efficiencies.

To date, three candidate light-engine architectures have been proposed and demonstrated. Lasers can be used as light sources for conventional imaging architectures, illuminating a small amplitude-modulating liquid-crystal–on–silicon (LCOS) panel and typically employing *f*/2 relay optics to magnify the resultant field.[1,2] It is also possible to use an LCOS panel in phase-modulating mode, where a fast panel is used to show sets of diffraction patterns which are subsequently demagnified by projection optics.[3] Finally, scanned-beam architectures employ a rather different approach, using a rapidly moving silicon micromirror to mechanically deflect a laser spot across the image in a manner somewhat analogous to a cathode-ray-tube (CRT) system.

A great deal of interest has surrounded scanned-beam systems, in particular, due in part to the potential for extreme miniaturization and high optical efficiency. A number of limitations of such systems have recently become apparent, however, with laser speckle,[4] limited brightness, and high cost[5] being principal objections. In addition, it is clear that considerable confusion remains regarding the laser safety classification of scanned-beam projection displays and the implications for the achievable brightness roadmap of such systems.

In this paper, a model consistent with the IEC 60825-1 laser safety standard is used to derive the output power restrictions imposed by Class 1 and Class 2 laser safety classes upon scanned-beam projection display systems and the D65 white-balanced luminous flux values that would result.

2 Analysis methodology

As stated by IEC 60825-1,[6] the acceptable exposure limit for visible wavelength laser safety classification is determined by measuring in a limiting aperture of radius d = 7 mm, representative of the maximum dilation of the human eye, at a distance of r = 100 mm from the projection aperture. The measurement geometry is shown in Fig. 1.

Assuming that the power delivered to this aperture is measured over a classification period T_2, the maximum permissible optical power in the measurement aperture that a given laser safety standard allows is determined. By then inferring the total projected image power P_{image}, which would result in this condition and imposing a white-point condition, a photometric measure of maximum luminous flux L_{max} can be derived.

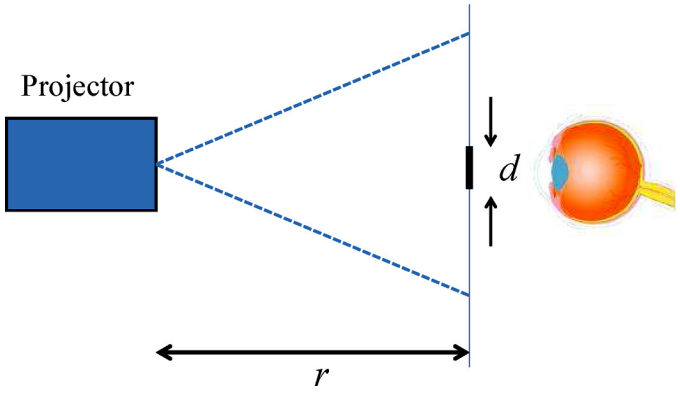

FIGURE 1 — Measurement geometry for determination of the laser safety classification.

Received 06/04/10; accepted 09/07/10.

The author is located at 310 E. San Rafael St., Colorado Springs, Springs, CO 80903, USA; telephone 719/434-1147, e-mail: ebuckley@ieee.org.

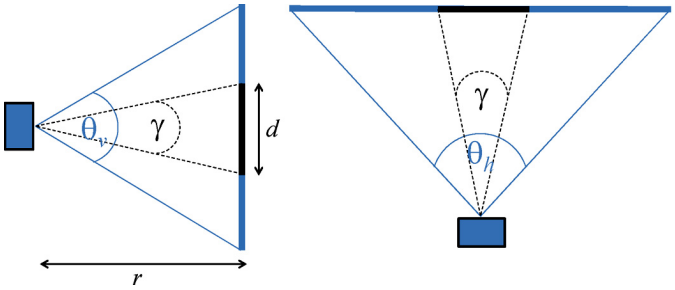

FIGURE 2 — Projection geometry for an image of extent $\theta_h \times \theta_v$ radians, containing the measurement aperture of diameter d and acceptance angle γ.

2.1 Projection geometry

In this study, both the projection and measurement geometries are independent of projection technology. A projection system with horizontal and vertical projection angles of θ_h and θ_v radians respectively gives rise to a rectilinear image at distance r containing the measurement aperture of diameter d, which is defined to have acceptance angle γ radians. The side and top views of the projection geometry are illustrated in Fig. 2. Without loss of generality, it is assumed that the horizontal and vertical projection angles contain M and N pixels, respectively.

The acceptance angle γ is related to the measurement aperture diameter d and measurement distance r by

$$\tan\left(\frac{\gamma}{2}\right) = \frac{d}{2r}. \tag{1}$$

2.2 General methodology

A given laser safety classification is defined by an acceptable exposure limit (AEL), which is dependent upon a number of physiological and technology-specific factors. The AEL is strongly influenced by the apparent source size, subtending an angle between α_{min} and α_{max} radians, which is particularly relevant to scanned-beam projectors in which the source size d_{spot} is effectively the diffraction-limited laser spot with size of the order of a millimeter. The AEL also depends upon an energy scaling factor pertaining to thermal retina damage, which, in turn, is weighted by the number and duration of modulated optical pulses delivered to the measurement aperture, and an exposure time t or classification time T_2. The generic eye-safety parameters defined by IEC 60825-1 are given in Table 1.

In general, there may be several AELs covering single pulse or pulse train conditions and photothermal or photochemical effects, so the limiting AEL is defined as the most restrictive of AEL_n, where $n = 1 \ldots N$, so that

$$AEL = \min\{AEL_1, AEL_2, \ldots, AEL_N\}. \tag{2}$$

The maximum power that can be delivered to the projected image P_{image} is then determined such that the energy at the measurement aperture $E_{aperture}$ is less than the AEL, thereby satisfying

$$E_{aperture} < AEL. \tag{3}$$

To calculate the maximum optical image power P_{image} that can be delivered while maintaining the appropriate AEL at the measurement aperture, the proportion of energy η delivered to the aperture in T_2 sec is calculated so that

$$E_{aperture} < T_2 \eta P_{image}, \tag{4}$$

where, neglecting any distortion in the image, the fraction of power delivered into the measurement aperture is given to a first-order approximation by

$$\eta \approx \frac{\gamma^2}{\theta_h \theta_v}. \tag{5}$$

As previously shown,[4] a scanned-beam system is not able to direct the entire laser-beam power into just one pixel due to limitations imposed by the maximum laser modulation frequency and the resonant nature of the MEMS mirrors employed. Hence, the worst-case situation for eye safety is derived from the full-white-screen condition; using this fact and combining Eqs. (3) and (4) gives the result that the radiometric power P_{image} exiting a scanned beam system should not exceed a limit defined by

$$P_{image} < \frac{AEL(J)}{T_2 \eta} \tag{6}$$

in order to satisfy a given laser safety classification.

2.3 Radiometric-to-photometric conversion

Since the aim of the paper is obtain a maximum luminous flux value for the given laser safety classification, it is necessary to convert the radiometric figure P_{image} [in for the total output of Eq. (11)] into photometric quantities for the red, green, and blue sources. Although the luminous-efficacy function $v(\lambda)$[7] can be used to convert the output power into luminous-flux values $L_{R,G,B}$, the process becomes compli-

TABLE 1 — Eye-safety parameters defined by IEC 60825-1.

Quantity	Symbol	Value	Source
Measurement aperture diameter (mm)	d	7	Ref. 6, p. 34, Table 10
Measurement aperture distance from source (mm)	r	100	Ref. 6, p. 34, Table 10
Minimum source angular subtense (mrad)	α_{min}	1.5	Ref. 6, p. 34, Table 10
Maximum source angular subtense (mrad)	α_{max}	100	Ref. 6, p. 35, 9.3(ii)
Aperture acceptance angle (rad)	γ	0.07	Eq. (1)

cated by the need to ensure the laser-power balance is consistent with a sensible white-point value.

To determine the respective laser powers which give a pre-determined white point, it is necessary to start from the definition of the CIE *XYZ* tristimulus functions, which are defined in terms of the color-matching functions $\bar{x}(\lambda)$, $\bar{y}(\lambda)$, $\bar{z}(\lambda)$, and a spectral power distribution $I(\lambda)$.[8]

$$X = \int_0^\infty I(\lambda)\bar{x}(\lambda)d\lambda,$$
$$Y = \int_0^\infty I(\lambda)\bar{y}(\lambda)d\lambda, \qquad (7)$$
$$Z = \int_0^\infty I(\lambda)\bar{z}(\lambda)d\lambda.$$

In this analysis, it is assumed that a D65 white point at a color temperature of 6500K is to be obtained from RGB laser sources of wavelengths λ_b = 445 nm, λ_g = 532 nm, and

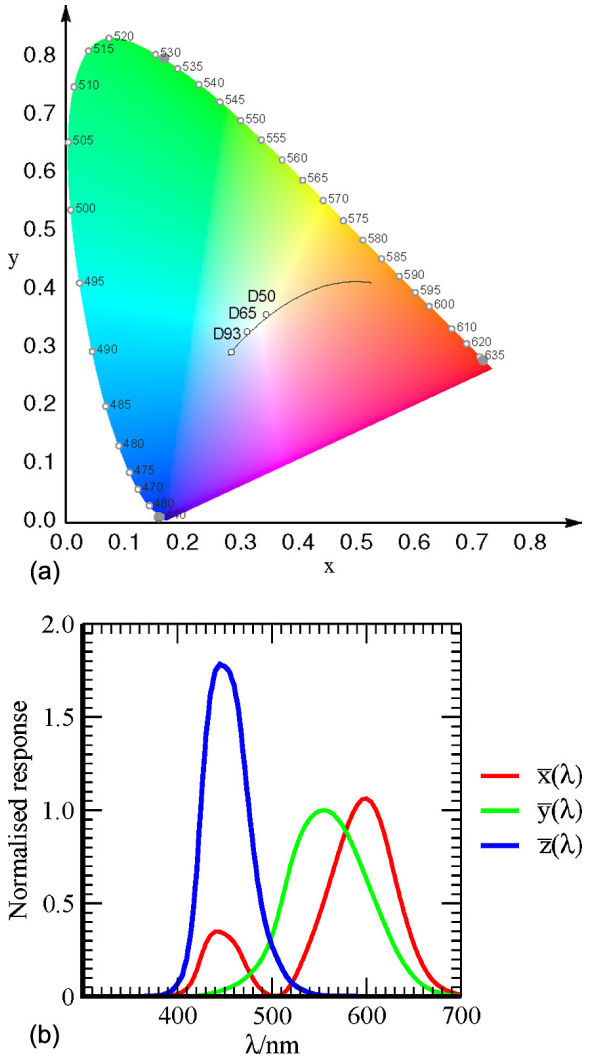

FIGURE 3 — (a) CIE 1931 color-space chromaticity diagram, showing white points and laser primary wavelengths. (b) The CIE standard observer color-matching functions $\bar{x}(\lambda)$, $\bar{y}(\lambda)$, $\bar{z}(\lambda)$.

TABLE 2 — Color-matching function values for the chosen laser primaries.

λ (nm)	$\bar{x}(\lambda)$	$\bar{y}(\lambda)$	$\bar{z}(\lambda)$
642	0.41209	0.15964	0.00001
532	0.18914	0.88496	0.03693
445	0.34806	0.02980	1.78260

λ_r = 642 nm such as those manufactured by Nichia,[9] Corning,[10] and Opnext,[11] respectively. The CIE standard observer color-matching functions are plotted in Fig. 3(b), and the color-matching function values (x, y, z) for the chosen laser primaries are shown in Table 2.

The tristimulus values of Eq. (7) can be converted to the (x, y, z) coordinates of the CIE color-space chromaticity diagram using the following equations:

$$x = \frac{X}{X+Y+Z},$$
$$y = \frac{Y}{X+Y+Z}, \qquad (8)$$
$$z = 1-x-y$$

and from the resultant CIE 1931 color-space diagram shown in Fig. 3(a), it is possible to determine the coordinates of the appropriate color point. For D65 white, the (x_w, y_w) white point chromaticity coordinates are (0.31271, 0.32902), giving (X, Y, Z) tristimulus values of (95.04, 100.00, 108.88).

Finally, the luminous flux for each color L_R, L_G, and L_B can then be calculated from the color-matching function values at each wavelength and color-matching functions at the prescribed white point using the following matrix operation[12]

$$\begin{bmatrix} L_R \\ L_G \\ L_B \end{bmatrix} = \begin{bmatrix} \frac{\bar{x}_r}{\bar{y}_R} & \frac{\bar{x}_G}{\bar{y}_G} & \frac{\bar{x}_B}{\bar{y}_B} \\ 1 & 1 & 1 \\ \frac{\bar{z}_r}{\bar{y}_t} & \frac{\bar{z}_g}{\bar{y}_g} & \frac{\bar{z}_b}{\bar{y}_b} \end{bmatrix}^{-1} \begin{bmatrix} X \\ Y \\ Z \end{bmatrix} \qquad (9)$$

and the ideal laser output powers P_R, P_G, and P_B can be calculated from the luminous-flux values using

$$\begin{bmatrix} P_R \\ P_G \\ P_B \end{bmatrix} = \frac{1}{683} \begin{bmatrix} \frac{L_R}{\bar{y}_r} \\ \frac{L_G}{\bar{y}_g} \\ \frac{L_B}{\bar{y}_b} \end{bmatrix}. \qquad (10)$$

3 Scanned-beam projector analysis

Having outlined the general measurement philosophy, the analysis proceeds by making some assumptions about the nature and performance of the projection system. A scanned beam system operates by spatially modulating red, green, and blue laser sources using one or two micromirror devices, with the spot resulting from the combination of the three

TABLE 3 — Summary of the system parameters for a WVGA scanned-beam projection system.

Quantity	Symbol	Value	Source
Horizontal resolution	M	850	Ref. 13
Vertical resolution	I	480	Ref. 13
Throw ratio	x/d	1	Ref. 13
Aspect ratio	r_a	16:9	Ref. 13
Refresh rate/Hz	f_r	60	Ref. 13
Beam diameter at measurement aperture/mm	D_{spot}	0.6	Ref. 14
Angular subtense of source/mrad	α	6	Eq. (11)
Horizontal throw angle/rad	θ_h	0.8	Eq. (13)
Vertical throw angle/rad	θ_v	0.48	Eq. (13)

wavelengths being scanned across the image. To achieve pixel definition, the lasers are pulsed rapidly. To provide gray scale, the red and blue semiconductor lasers are pulse-width modulated while limitations in the green laser-modulation bandwidth may necessitate analog modulation above and below threshold.

Due to the extremely high modulation frequency of the laser sources and the small beam diameters employed in the optical system, scanned-beam systems are not able to employ a diffuser. Although this makes speckle reduction in the system very difficult, the simplicity of the optical architecture eases the safety analysis. In such a system, the angular subtense of the apparent source α is simply given by

$$\tan(\alpha/2) = \frac{d_{spot}}{2r}, \tag{11}$$

where r is the distance to the measurement aperture and, due to the very high f-numbers inherent in scanned-beam architectures, the beam divergence can assumed to be zero.

For a given projection system, the image size in the plane of the measurement aperture, determined by the horizontal and vertical throw angles θ_h, and θ_v, is an important parameter in determining P_{image}. It is straightforward to show using a one-dimensional geometrical argument that the throw angle θ is related to the image size h and the projection distance x by

$$\tan\frac{\theta}{2} = \frac{h}{2x} \tag{12}$$

and when the projection distance x is approximately equal to the image diagonal size d, it follows that the throw angles and the aspect ratio r_a are related by

$$\begin{aligned} \tan\frac{\theta_h}{2} &= \frac{1}{2\sqrt{r_a^{-2}+1}}, \\ \tan\frac{\theta_v}{2} &= \frac{1}{2\sqrt{r_a^{2}+1}}. \end{aligned} \tag{13}$$

For the purposes of this analysis, a single-mirror scanned-beam projection system operating at WVGA resolution (850 × 480 pixels) and a frame rate of f_r = 60 Hz is assumed. The system parameters, assumed and calculated, are summarized in Table 3.

3.1 Class 2 operation analysis

The IEC 60825-1 standard defines the Class 2 AEL for an exposure time t, where $1.8\times10^{-5}\ s \leqq t \leqq 10$ sec and wavelength λ, where 400 nm $\leqq \lambda \leqq$ 700 nm, as

$$AEL = 7\times10^{-4}C_6 t^{0.75}\ \text{J}, \tag{14}$$

where C_6 is the effective source size correction factor given by

$$C_6 = \begin{cases} 1 & \alpha \le \alpha_{\min} \\ \alpha/\alpha_{\min} & \alpha_{\min} \le \alpha \le \alpha_{\max} \\ \alpha_{\max}/\alpha_{\min} & \alpha < \alpha_{\max} \end{cases} \tag{15}$$

and α is the angular subtense of the source defined in Eq. (11). The beam-correction factor for the scanned-beam system under analysis is found to be C_6 = 4.

3.1.1 Single-pulse analysis

According to Freeman,[14] a typical pulse width in a WVGA scanned-beam system is of the order of τ = 20 nsec, which IEC 90825-1 permits to be treated as a pulse of duration $t = T_i$ = 18 μsec in the visible region. For a single pulse, the maximum permissible power is equal to the AEL of Eq. (14) divided by T_i, and hence

$$AEL_1 = 7\times10^{-4}C_6 T_i^{-0.25}\ \text{W} \tag{16}$$

which results in P_{image} = 3.4 W, using Eq. (5) to account for the fractional aperture area. The relatively large value is due to the fact that Eq. (16) represents a thermal AEL and the radiometric power figure obtained corresponds to the small thermal hazard posed by one short pulse.

3.1.2 Pulse-train analysis

In a single-mirror scanned-beam projection system, the pulse width is determined by the behavior of the fast scan

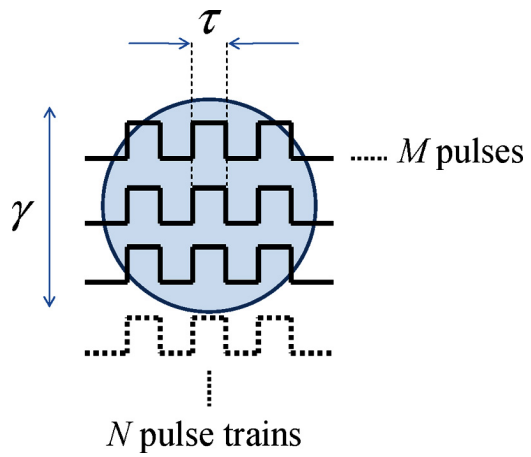

FIGURE 4 — Pulses of width τ, corresponding to a resolution of $N \times M$ pixels, incident upon a measurement aperture of acceptance angle γ.

axis which, in turn, corresponds to the horizontal resolution. Given pulses of approximately τ = 20 nsec duration, the total pulse on time τ_{tot} is determined by the number of horizontal pixels, throw angle, and aperture size so that

$$t_{tot} = \frac{\gamma M}{\theta_h} \cdot 20 \times 10^{-9} \tag{17}$$

neglecting mirror fly-back time between rows. Figure 4 depicts the relationship between the pulses of duration τ incident upon the measurement aperture of acceptance angle γ radians, and the horizontal and vertical resolution N and M, respectively.

Since t_{tot} is of the order of 1 μsec, all pulses in a horizontal line can therefore be grouped into a single pulse of duration T_i = 18 μsec according to IEC 60825-1. This dramatically simplifies the analysis since the duration T_i is now independent of the gray-scale modulation in each pulse, and all that remains is to determine how many times the scanned beam intercepts the measurement aperture in the vertical direction per one frame period.

This is trivial to calculate; since the fast scan direction is horizontal, and because all pulses in the measurement aperture count as one pulse of duration T_i, the number of pulses n' incident upon the aperture per frame is equal to the number of times the beam passes from the top of the aperture to bottom in one frame, or

$$n' = \frac{N\gamma}{\theta_v} \tag{18}$$

so that the total number of pulses incident upon the measurement aperture during the classification period T_2 is

$$n = n' f_r T_2. \tag{19}$$

In a scanned-beam system, the pulse duration is constant even though the pulse energy is not, since each pixel can take a different gray-scale value. In this case, the IEC standard allows the average value of the exposure to be compared with the AEL, and the presence of n pulses in the blink response time T_2 = 0.25 sec is accounted for by multiplying Eq. (16) by $n^{-0.25}$ (Ref. 6, p. 31). The final expression for the AEL then becomes

$$\begin{aligned} \frac{AEL_2}{n} &= 7 \times 10^{-4} C_6 \frac{T_i^{0.75}}{T_2} \times n^{-0.25} \text{ W}, \\ \therefore AEL_2 &= 7 \times 10^{-4} C_6 \frac{(nT_i)^{0.75}}{T_2} \text{ W}, \end{aligned} \tag{20}$$

from which the radiometric image limit P_{image} = 46 mW can be obtained. [IEC 60825-1 also allows the use of the total on-time-pulse (TOTP) method, in which the AEL is determined by the sum of all pulse durations within the emission duration T_2; in this way, the same result for Eq. (20) can be obtained by setting the total on-time $t = NT_i$ in Eq. (16).[15]]

At some 74 times smaller than AEL_1, this is clearly the limiting case for Class 2 classification. Equations (7)–(10) can be used to calculate a D65 white-balanced luminous flux of ≈11 lm corresponding to this radiometric power limit. A summary of the relevant parameter values for the Class 2 safety analysis is provided in Table 4.

3.2 Class 1 operation analysis

In certain situations, for example in the case of young children where the blink response may not be fully developed or when an observer has dark-adapted eyes, it may not be possible to assume a blink-response-limited classification period of T_2 = 0.25 sec. In this case, it is necessary to consider the requirements imposed by a Class 1 safety classification in which the exposure time is t = 100 sec for 400 nm ≦ λ ≦ 700 nm and a source of angular extent greater than 1.5 mrad.[6]

TABLE 4 — Summary of relevant parameter values for the Class 2 safety analysis.

Quantity	Symbol	Value	Source
Blink response classification time/sec	T_2	0.25	Ref. 6, p. 30, 8.4(e) condition (i)
Source size correction factor	C_6	4.0	Ref. 6, p. 39, Table 4 and Eq.(15)
Effective pulse duration/μsec	T_i	18.0	Ref. 6, p. 31,Table 9
No. pulses incident upon measurement aperture	n	1050	Eq.(18)
Acceptable exposure limit/mW	AEL_1	43.0	Ref. 6, p. 36, Table 2 and Eq.(16)
Acceptable exposure limit/mW	AEL_2	0.57	Ref. 6, p. 36, Table 2 and Eq.(20)
Maximum radiometric power at aperture/mW	P_{image}	46.8	Eqs. (6), (16), and (20)
Maximum luminous flux at aperture/Lm	L_{max}	11.2	Eqs. (6), (7)–(10), and (20)

For a wavelength range 400 nm = λ = 1400 nm, the classification period T_2 is then defined as

$$T_2(s)=\begin{cases}10 & \alpha<1.5\ \text{mrad}\\ 10\times10^{\left\lceil\frac{(\alpha-\alpha_{\min})}{98.5}\right\rceil} & 1.5\ \text{mrad}<\alpha<100\ \text{mrad},\\ 100 & \alpha>100\ \text{mrad}\end{cases} \quad (21)$$

which, given the scanned-beam system parameters of Table 4, gives $T_2 \approx 11$ sec.

The analysis of Class 1 laser safety is further complicated since, in addition to the thermal limits, photochemical-based restrictions apply for the green and blue wavelengths λ_g and λ_b, which are weighted by the function C_3, where

$$C_3(\lambda)=10^{0.02(\lambda-450)} \quad (22)$$

for 400 nm ≦ λ ≦ 700 nm.

To determine a radiometric power figure that satisfies the Class 1 classification requires that the photochemical power at the output of the projector for blue and green wavelengths, and the photothermal power summed across all wavelengths, are less than the respective limits. Expressed mathematically, if the photochemical limits at blue and green wavelengths are $P_{ph}(\lambda_b)$ and $P_{ph}(\lambda_g)$, respectively, and the photothermal output power limit is P_{th}, then to achieve a Class 1 the following must simultaneously hold:

$$\begin{aligned}P_b &< P_{ph}(\lambda_b),\\ P_g &< P_{ph}(\lambda_g),\end{aligned} \quad (23)$$

and

$$P_{image} < P_{th}. \quad (24)$$

3.2.1 Photochemical hazard

The AEL for the photochemical hazard for t = 100 sec and a source angular subtense of α = 11 mrad is given by

$$AEL_{b,g}=3.9\times10^{-3}C_3\left(\lambda_b,\lambda_g\right)\ \text{J} \quad (25)$$

which, for a single pulse and α ≠11 mrad, gives a photochemical power limit of

$$P_{b,g}=\left(\frac{\alpha}{11}\right)^2\frac{AEL_{b,g}}{\eta t}W \quad (26)$$

in the 7-mm measurement aperture. For green and blue wavelengths, respectively, the Class 1 photochemical power limits are approximately P_g = 40 mW and P_b = 1 mW.

3.2.2 Photothermal hazard

For a source of angular subtense α > 1.5 mrad, there are two formulae for the AEL depending upon the classification and emission duration T_2 and t, respectively:

$$AEL=\begin{cases}7\times10^{-4}C_6T_2^{-0.25}(\text{W}) & t>T_2\\ 7\times10^{-4}C_6t^{-0.25}(\text{J}) & t\le T_2\end{cases}. \quad (27)$$

For continuous-wave (CW) emission, t = 100 sec and $T_2 \approx 11$ sec so the first of these conditions apply. For single-pulse and pulse-train conditions, however, the photothermal AEL is determined by $t = T_i < T_2$ and the second condition is used. The analysis proceeds in a similar fashion to Sec. 3.1, with the only difference being the new value for T_2. Hence, the approximate radiometric power limits are P_{image} = 0.15 mW, P_{image} = 10 mW, and P_{image} = 120 mW for CW, pulse-train, and single-pulse conditions, respectively.

A summary of the results and relevant simulation parameters for the Class 1 analysis are summarized in Table 5.

An iterative method was used to find the radiometric image power limit that satisfied Eqs. (23) and (24) in the pulse-train mode of operation representative of a scanned-beam system. Since the limiting AEL is determined by the photochemical hazard in the blue wavelength, the resultant maximum image brightness L_{max} was found to be just 1 lm.

4 Summary

This paper has shown that scanned-beam systems are fundamentally limited in terms of maximum achievable luminous

TABLE 5 — Summary of the relevant parameter values for the Class 2 safety analysis.

Quantity	Symbol	Value	Source
Emission duration/sec	t	100	Ref. 6, p. 30, 8.4(e) condition (ii)
Photochemical wavelength correction factor	$C_3(\lambda)$	λ = 445, $C_3 \approx 1$ λ = 532, $C_3 \approx 44$	Ref. 6, p. 39, Table 4
Classification period/sec	T_2	11.1	Ref. 6, p. 39, Table 4, Eq. (21)
Angle of acceptance/mrad	γ	11	Ref. 6, p. 34, 9.3(c)
Photochemical power limit at aperture/mW	P_g P_b	39.7 0.91	Eq. (26)
Photothermal power limit at aperture/mW	P_{th}	0.15 (CW) 10.3 (pulse-train) 120 (single pulse)	Eq. (27)
Maximum radiometric power at aperture/mW	P_{image}	0.91	Eqs. (23) and (24)
Maximum luminous flux at aperture/Lm	L_{image}	1.0	Eqs. (6), (7)–(10)

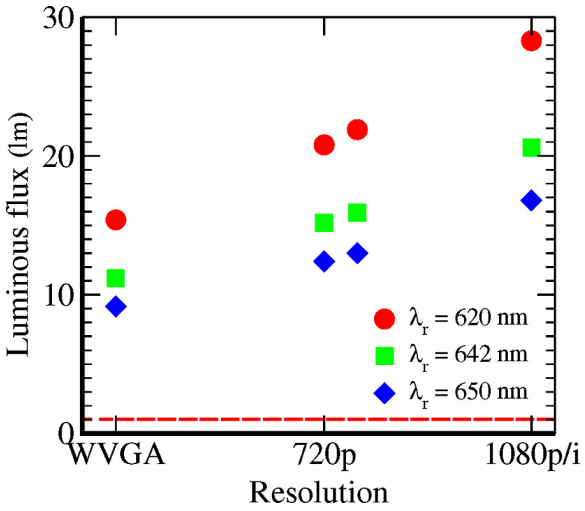

FIGURE 5 — Maximum achievable D65 white-balanced luminous flux for Class 1 (dotted line) and Class 2 operation, as a function of red source wavelength and resolution with constant aspect ratio.

flux, principally because of the very small effective source size. To achieve a Class 1 classification, the D65 white balanced luminous flux emitted by a WVGA single-mirror scanned beam system is limited to approximately 1 lm, while the corresponding Class 2 limitation is roughly 11 lm. It is clear, therefore, that the photochemical hazard at blue wavelengths prevents the realization of a practical Class 1 scanned-beam system.

The achievable Class 2 D65 luminous flux can be increased slightly in a number of ways. The higher luminous efficacy of sources at shorter red wavelengths can be exploited to produce a higher photometric power for the same radiometric power, so using a source with λ_r = 635 nm would then result in an upper limit of 12.7 lm for a WVGA system. Unfortunately, this strategy may be counterproductive for applications requiring low power consumption since electrical-to-optical conversion efficiencies of 635-nm devices tend to be lower due to heating effects in AlGaInP layers at shorter wavelengths.[16]

Brightness can also be increased by increasing the number of vertical lines, as per Eq. (18); as Fig. 5 demonstrates, in which the maximum Class 2 brightness is evaluated at resolutions of similar aspect ratio, a 720p system could emit a maximum of 15.2 lm while remaining a Class 2 system. While this appears to be an attractive way for manufacturers of scanned-beam systems to simultaneously improve two aspects of system performance, this approach is fundamentally compromised for low-power applications since the concomitantly increased laser modulation frequency increases power consumption in the laser itself[10] as well as in the associated analog drive electronics. Limitations in the frequency-doubled green laser modulation frequency also appear to place an upper limit on the achievable resolution at WXGA.[17] Nevertheless, a 720p system using 635-nm red laser illumination could feasibly reach 17 lm while remaining Class 2 eye safe. A range of Class 2 eye-safe luminous-flux values, plotted as a function of resolution and red source wavelength, are provided in Fig. 5.

Finally, it may also be possible to relax the maximum brightness limitation by increasing the horizontal and vertical throw angles. However, since noticeable image distortion is already evident in scanned-beam systems, it is clear that projection angles achievable using commercially available bulk silicon MEMS systems are likely to be limited to the ranges considered in this study for the foreseeable future, although carbon-fiber-based MEMS structures[18] show promise in this regard.

In conclusion, it can be reasonably stated that the useful range of the D65 white-balanced luminous flux obtainable from scanned-beam systems whilst maintaining a Class 2 eye-safety classification is between 10 and 17 lm, based on nominal resolutions between WVGA and 720p, and red laser wavelengths in the range 635–642 nm. It remains to be seen whether this class of device can remain competitive with LED-based WVGA products capable of producing 15 lm,[19] the expected emergence of 20-lm 720p systems in late 2010,[20] and the existence of LCOS-based laser-projection products which are already demonstrating Class 1 eye-safety performance at 15[21] and 20 lm.[22]

References

1 D. Darmon *et al.*, "LED-illuminated pico-projector architectures," *SID Symposium Digest*, **39**, 1070–1073 (2008).
2 K. Guttag *et al.*, "854 × 600 pixel LCOS microdisplay with 5.4 µm pixel pitch for pico-projectors," *Proc. IDW '08* (2008).
3 E. Buckley, "Holographic laser projection technology," *SID Symposium Digest* **39**, 1074–1078 (2008).
4 E. Buckley, "Holographic laser projection technology (invited article)," *Information Display* **24**, No. 12, 22–25 (December 2008).
5 Insight Media LLC, *Picoprojector Report*, 119 (October 2009).
6 *Safety of laser products – Part 1: Equipment classification, requirements and user's guide*, British Standards Institute Std. BS EN 60825-1 (1994).
7 CIE, *Proc. Commission Internationale de l'Eclairage* (Cambridge University Press, Cambridge, U.K., 1924).
8 T. Smith and J. Guild, "The CIE colorimetric standards and their use," *Trans. Opt. Soc. London*, No. 33, 73–134 (1931–1932).
9 Nichia, "Blue laser diode NDHB510APA datasheet." [Online]. Available: http://www.nichia.co.jp/specification/en/product/ld/NDHB510APA-E.pdf.
10 V. Bhatia *et al.*, "High efficiency green lasers for mobile projectors," *Proc. IDW '07* (2007).
11 Opnext, "HL6364DG/65DG datasheet," May 2006. [Online]. Available: http://www.photonic-products.com/products/laserdiodes_visible/opnext/hl6364dg_65dg.pdf.
12 D. Armitage *et al.*, *Introduction to Microdisplays* (John Wiley and Sons, West Sussex, 2006), Chap. 10: Projection Displays, p. 310.
13 Microvision Inc., "ShowWX laser pico projector specifications," May 2010. [Online]. Available: http://www.microvision.com/showwx/specs.html.
14 M. Freeman *et al.*, "Scanned laser pico-projectors: Seeing the big picture (with a small device)," *Opt. Photon. News* **20**, No. 5, 28–34 (2009).
15 A. R. Henderson and K. Schulmeister, *Laser Safety* (Taylor and Francis Group, LLC, 2004).
16 Sony Corp., "The science of the laser projector," October 2009. [Online]. Available: http://www.sonyinsider.com/2009/10/12/the-science-of-the-laser-projector/.
17 Corning, Inc., "Corning Green Laser G-2000 Module," 2010. [Online]. Available: http://www.corning.com/WorkArea/linkit.aspx?LinkIdentifier=id&ItemID=32243.

18 Mezmeriz, Inc., "Carbon fiber MEMS micromirrors: enabling the next generation of picoprojectors," September 2008. [Online]. Available: http://www.memsinfo.jp/whitepaper/730.pdf.
19 Texas Instruments, "Press release," January 2010. [Online]. Available: http://www.dlp.com/technology/dlp-press-releases/press-release.aspx?id=1369.
20 K. Guttag, "High-resolution microdisplays for pico-projectors (invited paper)," *SID Symposium Digest* **41**, 1057–1060 (2010).
21 Light Blue Optics Inc., "Light Touch specifications," February 2010. [Online]. Available: http://www.lightblueoptics.com/products/light-touch/specifications/.
22 Aaxa technologies, "Press release," February 2010. [Online]. Available: http://www.aaxatech.com/news/l1_laser_pico_projector.html.